Benchtop chemistry for the rapid prototyping of label-free biosensors: Transmission localized surface plasmon resonance platforms

Wei-Ssu Liao, Xin Chen, Tinglu Yang, Edward T. Castellana,
Jixin Chen, and Paul S. Cremer[a]
Department of Chemistry, Texas A&M University, College Station, Texas 77843

Herein, a simple label-free biosensor fabrication method is demonstrated based on transmission localized surface plasmon resonance (T-LSPR). The platform, which consists of a silver nanoparticle array, can be prepared in just a few minutes using benchtop chemistry. The array was made by a templating technique in conjunction with the photoreduction of Ag ions from solution. This metal surface was functionalized with biotin-linked thiol ligands for binding streptavidin molecules from solution. For an array of 19 nm diameter silver nanoparticles, a redshift in the T-LSPR spectrum of 24 nm was observed upon protein-ligand binding at saturation. The binding constant was found to be 2×10^{12} M^{-1}. Platforms were also fabricated with silver nanoparticles of 34, 55, and 72 nm diameters. The maximum LSPR wavelength shift was nanoparticle size dependent and the maximum sensitivity was obtained with the smaller nanoparticles. © *2009 American Vacuum Society.* [DOI: 10.1116/1.3284738]

I. INTRODUCTION

Surface plasmon resonance (SPR) techniques have recently become popular methods for designing chemical and biological sensors because they afford label-free detection with relatively highly sensitivity.[1–5] Classical SPR applications exploit refractive index changes in the sensor/fluid interface to detect analyte molecules.[6–10] The typical reflectometry setup, however, somewhat limits the widespread employment of this type of platform. Recently, a simpler setup, transmission localized surface plasmon resonance, has been demonstrated.[11–16] Transmission localized surface plasmon resonance (T-LSPR) can be achieved with noble metal nanoparticles spread on a transparent substrate. The nanoparticle surface conduction electrons collectively oscillate when an electromagnetic wave is introduced. This coherent oscillation can induce photon absorption and scattering, both of which are very sensitive to the dielectric properties of the surrounding medium.[15,17] This effect is typically present only when the metal particle size is smaller than the wavelength of the incident light. Moreover, this optical phenomenon is strongly sensitive to nanoparticle size, shape, and composition.[18–20]

In previous T-LSPR work, Okamoto *et al.*[11] used colloidal gold nanoparticles spread on glass substrates for sensing polymer coatings. Rubinstein and co-workers[12,21–23] demonstrated the use of evaporated gold island films for chemical sensing. Malinsky *et al.*[13] employed silver nanotriangles fabricated by nanosphere lithography for sensing proteins. Chilkoti and co-workers[14,24–26] demonstrated successful colloidal gold nanoparticle and nanorod transmission T-LSPR biosensors, while Dahlin *et al.*,[27] Sharpe *et al.*,[28] and Brolo *et al.*[29,30] utilized nanohole features as biosensing arrays.

Other researchers also employed similar transmission approaches for mono-/multilayer film sensing.[11,12,21–23] This includes protein binding assays,[13,14,17,18,31] DNA hybridization assays,[32,33] as well as polymer studies.[34]

Because a conventional UV-visible spectrometer can be employed with the T-LSPR approach, biosensing becomes more convenient. Nevertheless, the fabrication of the sensing platforms itself can still be an elaborate and time-consuming process. Therefore, there is significant impetus to designing a simple, inexpensive, and rapid method for creating metal nanoparticles arrays, which could maintain high sensitivity for the detection of biomolecules.

We have recently demonstrated a rapid prototyping approach for the fabrication of nearly monodisperse silver nanoparticle arrays on TiO$_2$ thin films.[35] TiO$_2$ is a well-studied photocatalyst, which has been widely used for metal nanoparticle preparation.[36–43] The process involves the photoreduction of metal ions by UV illumination of the oxide thin film.[36,37,41–44] The size, shape, and density of the metal nanoparticles in these studies could be well controlled by using nanoporous alumina filtration membranes as templates. The alumina template confined the size and shape of the nanoparticles during their production. The entire fabrication process could be completed rapidly at a standard benchtop without the need for vacuum techniques or a clean-room environment. Moreover, metal particles in the size range of 10–100 nm could be easily produced using this technique.

We reasoned that our metal nanoparticle arrays should be a convenient platform for creating T-LSPR biosensor substrates (Fig. 1). To investigate this, a monodisperse silver nanoparticle array was fabricated by the templated photoreduction process and then treated with a ligand-linked thiol for protein capture from solution. The well-studied biotin/streptavidin binding pair was chosen for this purpose. It was found that the size of the silver nanoparticles employed was critical for obtaining high quality binding data. Specifically,

---

[a]Author to whom correspondence should be addressed; electronic mail: cremer@mail.chem.tamu.edu
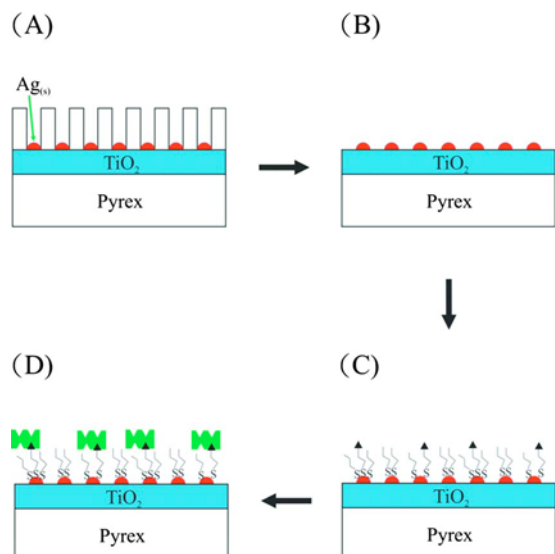
FIG. 1. (Color online) Schematic of the process for fabricating monodisperse silver nanoparticle based T-LSPR biosensors. (a) Silver nanoparticle array templated by an alumina membrane on a thin TiO_2 film during the photoreduction process. (b) Monodisperse silver nanoparticle array after alumina membrane lift off. (c) Biotin/PEG modified silver nanoparticle biosensing array. (d) Binding of streptavidin molecules.

smaller particles (19 or 34 nm), which exhibited narrower plasmon bands, were found to be superior to larger particles (>50 nm). The platforms that were employed have some of the narrowest size distributions for particle arrays used to date for protein detection. The results clearly demonstrated that excellent sensitivity from a single layer of metal particles could be achieved. In fact, quantitative equilibrium dissociation constant data could also be abstracted.

## II. EXPERIMENTAL SECTION

A. Materials

Polished Pyrex 7740 wafers (25.4 mm^2 and 0.5 mm thick) were purchased from Precision Glass and Optics (Santa Ana, CA) and nanoporous alumina filtration membrane templates came from Synkera Technologies (Longmont, CO). The nanotemplates had pore sizes of 18, 35, 55, and 73 nm (1.3 cm diameter and 50 μm thickness). The templates had pore densities of 5×10^{10}, 1×10^{10}, 5×10^9, and 4×10^9 pores/cm^2, respectively, according to the manufacturer. We confirmed these values in house by scanning electron microscopy (Zeiss 1530 VP FE-SEM). Titanium (IV) isopropoxide, $AgNO_3$, 4-(2-hydroxyethyl) piperazine-1-ethane sulfonic acid (HEPES buffer salt), bovine serum albumin (BSA), sodium phosphate, and sodium chloride were purchased from Sigma-Aldrich (Milwaukee, WI). HCl was purchased from EM Industries (Gibbstown, NJ) and isopropanol was purchased from Acros (Geel, Belgium). Ethanol was obtained from AAPER Alcohol and Chemical Co. (Shelbyville, KY). Purified water ($\geq$18.2 MΩ cm) was prepared with a NANOpure Ultrapure Water System (Barnstead, Dubuque, IA). H_2O_2 and H_2SO_4 were purchased from EMD Chemicals Inc. (Gibbstown, NJ).

Biotin poly(ethylene glycol) (PEG) disulfide (structure 1) and PEG propionate disulfide (structure 2) were obtained from BioVectra Inc. (Prince Edward Island, Canada). Although drawn in the protonated state, it should be noted that structure 2 will lead to a net negative charge at the aqueous/ nanoparticle interface under the conditions of our experiments. Streptavidin and Texas Red-labeled streptavidin were purchased from Invitrogen (Eugene, OR).

Structure 1: Biotin PEG disulfide
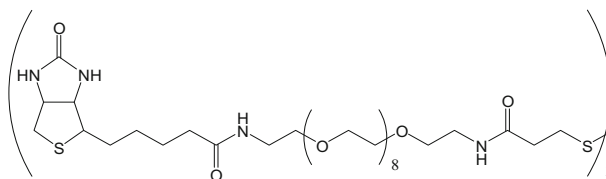
Structure 2: PEG propionate disulfide
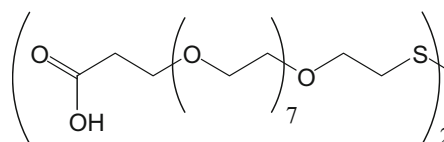
B. Solution preparation

HEPES buffer solution was made with purified water (10 mM, *p*H 7.4), while 10 mM phosphate buffered saline (PBS) was prepared with purified water at *p*H 7.2. Biotin PEG disulfide and PEG propionate disulfide solutions were made as 2 and 10 mg/ml stock solutions in HEPES buffer, respectively. These solutions were prepared immediately before use. The streptavidin, Texas Red-labeled streptavidin, and BSA solutions were prepared in PBS buffer as stock solutions at 1 mg/ml before dilution to the appropriate concentration.

C. Preparation of biosensor substrates

A transparent Pyrex wafer was used as the substrate and was cleaned in piranha solution (1:3 ratio of 30% H_2O_2 and H_2SO_4) to remove organic contaminants from the surface. Caution: piranha solution is a vigorous oxidant and should be used with extreme care. Next, the substrate was rinsed with copious amounts of purified water and dried with nitrogen gas. At this point, ~150 μl of a TiO_2 precursor solution was deposited onto the surface of the slide with a pipette. This solution was made from 1 g of titanium (IV) isopropoxide, 0.15 g of concentrated (37%) HCl, and 8.0 g of isopropanol. Next, a nanoporous alumina filtration membrane was placed on top of the solution-covered Pyrex slide and the liquid was allowed to evaporate under ambient conditions for 6 min. Following this, 300 μl of 0.1 M $AgNO_3$ solution was immediately introduced to the top side of the alumina membrane and the entire system was exposed to UV irradiation, which was applied through the Pyrex side for 5 min. This was done with a standard 500 W mercury arc lamp (Newport Oriel Instruments, Stratford, CT). After photoreduction in the metal particles onto the TiO_2 thin film, the alumina template was gently peeled away and the supported silver nanoparticle

array was washed with ethanol and purified water. The entire preparation procedure took 11 min to perform.

Once the sensor platform was formed, it was immediately incubated in a solution containing 0.5 mg/ml biotin PEG disulfide and 5.0 mg/ml PEG propionate disulfide (10 mM HEPES, *p*H 7.4) for several hours.[43] The PEG was employed to passivate nonspecific adsorption sites on the sensor surface. To prevent oxidation of the biotin molecules, the incubation was performed in the dark and the solution was surrounded by a N_2 atmosphere. This also helped prevent oxidation of the Ag nanoparticles. Finally, the nanosensor array was washed with ethanol and distilled water. At this point it was ready for protein biosensing.

Fluorescence control experiments were performed to ensure that biotin was appropriately presented on the nanoparticle array. A 1.0 μM solution of Texas Red-labeled streptavidin was introduced above the sample, incubated for 30 min, and then washed away with HEPES buffer. A strong fluorescent signal was detected from the sensing platform under an upright fluorescence microscope (Eclipse E800, Nikon). The fluorescence response was almost completely absent when a similar system was placed under a fluorescence microscope without the presence of biotin ligands at the interface.

D. SPR measurements and substrate imaging

Atomic force microscopy (AFM) measurements of Ag nanoparticle arrays were made with a Nanoscope IIIa from Digital Instruments (Santa Barbara, CA). These experiments were done in tapping mode in air with a type E scanner employing etched silicon tips (NSC15/No Al, Mikro Masch, Wilsonville, OR). UV-visible spectra were taken with a Lambda 35 UV/visible spectrometer (PerkinElmer Instruments, Shelton, CT). Since the Pyrex substrates were transparent, the chips could be directly and conveniently seated inside the spectrometer.

III. RESULTS

A. T-LSPR spectra of monodisperse Ag nanoparticle arrays

In a first set of experiments, a silver nanoparticle array was prepared with an alumina membrane template containing 18 nm pores. These pores were roughly hexagonally arrayed. The half sphere-shaped nanoparticles were quite uniform and had an average full width at half height (FWHH) at their base of $\sim 19 \pm 3$ nm according to AFM measurements in agreement with previous studies (data not shown).[35] The nearly monodisperse supported particle array was then tested for T-LSPR. The absorption peak at 480 nm in the UV-visible spectrum [Fig. 2(b)] is consistent with the plasmon resonance of Ag nanoparticles reported in literature.[44–46] It suggests that the SPR properties of the Ag nanoparticles are not significantly changed by the TiO_2 substrate. It should also be noted that bare TiO_2 surfaces had no such absorption feature in this frequency range [Fig. 2(a)].
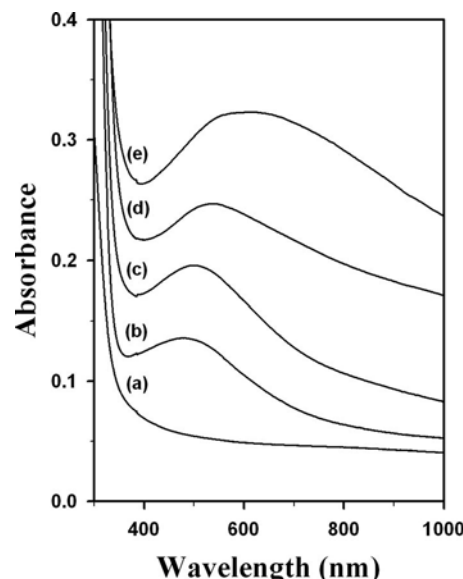

FIG. 2. UV/visible spectra of (a) a bare TiO_2 background and four different diameter silver nanoparticle arrays fabricated by (b) 18 nm, (c) 35 nm, (d) 55 nm, and (e) 73 nm templates, respectively.

Arrays with silver nanoparticles of different sizes were fabricated by using nanoporous alumina templates with different pore sizes (35, 55, and 73 nm). AFM data for these arrays looked essentially identical to those found previously by employing this templating method.[35] The silver nanoparticles that were produced had average particle sizes (FWHH) of 34 ± 3, 55 ± 6, and 72 ± 7 nm, respectively. The plasmon resonance absorption peak was found to redshift with increasing size of the Ag nanoparticles (Fig. 2). Moreover, the peak intensity increased and the peak width broadened with increasing particle size. Such observations are consistent with theory.[47–49] Indeed, the redshift of the absorption with increasing nanoparticle size is thought to be a quantum confinement effect. Both the dipole and quadrupole resonance modes should contribute to the peak and the resonance of the quadrupole moment should appear at shorter wavelength than that of the dipole moment.[50,51] Moreover, the contribution from the quadrupole resonance modes increases with the size of the nanoparticles. This is a significant factor in the peak broadening.[50–54] Here we demonstrated that such spectral properties can be achieved with nanoparticles made by a very simple rapid prototyping method. In fact, the optical properties appear to be comparable to, if not better than, those obtained with metal particles which were fabricated by more complex, expensive, and time-consuming processes.

B. T-LSPR biosensors

The monodisperse Ag nanoparticle array was incubated for several hours in a solution containing 0.5 mg/ml biotin PEG disulfide and 5 mg/ml PEG propionate disulfide in 10 mM HEPES buffer (*p*H 7.4) to obtain a biotin terminated surface, as shown schematically in Fig. 1(c). This represents a nominal ratio of biotin in background PEG of 1:10. The modified nanoparticle array was then incubated with strepta-
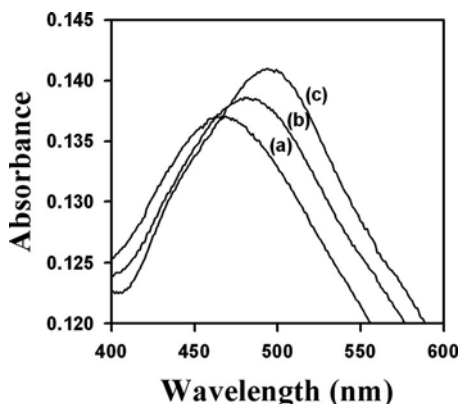
FIG. 3. UV/visible spectra of 19 nm diameter Ag nanoparticle biosensor array (a) before and after incubated with (b) 10^{-12} M and (c) 10^{-6} M streptavidin solutions, respectively.

vidin solutions of varying concentrations for 30 min. Absorption spectra were taken before and after incubation. Figure 3 shows representative experiments performed with a 19 nm silver nanoparticle array. It was found that the plasmon band redshifted upon protein adsorption until the surface was saturated with protein. We also noted in most experiments that the plasmon peak intensity increased upon adsorption; however, the peak intensity was not as reliable an indicator of protein binding as the frequency shift, in agreement with previous studies.[31]

Figure 4 shows the associate shift in peak frequency for the plasmon band as a function of streptavidin concentration for the 19 nm diameter Ag nanoparticles. Data were taken in a protein concentration range from 10^{-16} M to 10^{-6} M. In order to achieve equilibrium, all the protein incubation experiments were performed in a dark, hermetically sealed environment for a minimum of 3 h.[22] At the lowest protein concentration (10^{-16} M), the solution was incubated for 24 h to ensure equilibrium binding had been achieved. As can be seen from the data, the plasmon resonance shifted with increasing protein concentration and a simple Langmuir isotherm could be used to fit the data,[31]
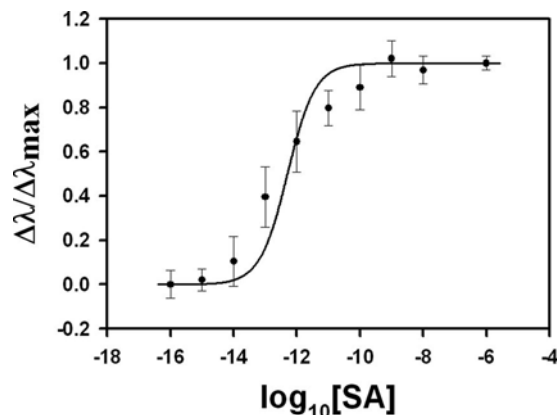

FIG. 4. Binding curve of the biotin-streptavidin interaction using a 19 nm diameter Ag nanoparticle sensor array. The solid dots represent experimental points while the curve represents the fit to a Langmuir isotherm.

$$\Delta\lambda/\Delta\lambda_{\max} = K[\mathrm{SA}]/(1 + K[\mathrm{SA}]),$$

where $\Delta\lambda$ is the wavelength shift caused by the addition of protein and $\Delta\lambda_{\max}$ is the wavelength shift which was observed at saturation. K is the apparent equilibrium association constant and $[\mathrm{SA}]$ is the concentration of streptavidin applied to the system. Using this equation gave a fitted value of $K = 2 \times 10^{12}$ M^{-1}, which is in rough agreement, although slightly weaker than literature data for similar systems measured by complementary methods (Green and Campbell: $\sim 10^{13}$ M^{-1}, Chilkoti and Stayton: 2.5×10^{13} M^{-1}).[55–60] In the present case, the binding constant is probably somewhat weakened because the negatively charged surface slightly destabilizes the bound state of the negatively charged streptavidin molecules.

Several control experiments were run to ensure that the data in Fig. 4 were not the result of nonspecific adsorption. First, 1 mg/ml BSA in PBS buffer (10 mM PBS, *p*H 7.2) was introduced to the biotin-PEG-conjugated 19 nm silver nanoparticle array. Very little, if any, discernable SPR peak shift was observed under these conditions ($\Delta\lambda = 1.0 \pm 1.0$ nm, three trials). In a second control experiment, a 5 mg/ml PEG propionate disulfide solution was incubated over a Ag nanoparticle array in the absence of biotinylated ligands. This system was challenged with a 10^{-6} M streptavidin solution for 30 min. Again, little evidence for a SPR shift could be found within experimental error ($\Delta\lambda = 0.0 \pm 1.0$ nm, three trials). Therefore, as expected, nonspecific binding of protein molecules on the PEG-covered nanoparticles was found to be quite low.[43]

By applying the same preparation methods, different diameter silver nanoparticle biosensors were also examined. Significantly, the sensitivity of the sliver nanoparticle sensors was particle size dependent. Figure 5 shows the absorption spectra of silver nanoparticle biosensors prepared by the same procedures as the 19 nm Ag nanoparticle array, but with 34, 55, and 72 nm nanoparticles, respectively. Absorption data are displayed both before and after a 30 min incubation of the sensor platform with a 1.0 μM streptavidin solution. This concentration should be more than enough to cause saturation binding under the conditions employed. As can be seen, protein binding caused a redshift in the plasmon resonance frequency for all three diameters of Ag nanoparticles. However, the magnitude of the red shift, $\Delta\lambda_{\max}$, was clearly size dependent. Specifically, a very distinct decrease in $\Delta\lambda_{\max}$ was observed with increasing metal particle size. This is consistent with the notion that the resonant electric field falls off faster with distance from the surface for smaller particles.[61] Hence, these nanoparticles are more sensitive to changes in refractive index within the first few nanometers of the surface. The values of $\Delta\lambda_{\max}$ as a function of size are provided in Table I. As can be seen, the shift is nearly same for the 19 and 34 nm arrays. The shift, however, drops dramatically as the size increased further, suggesting that larger particles become increasingly less useful as T-LSPR sensors. This was the case in spite of the fact that the absorption increased with the size of the nanoparticles (Table I). There-
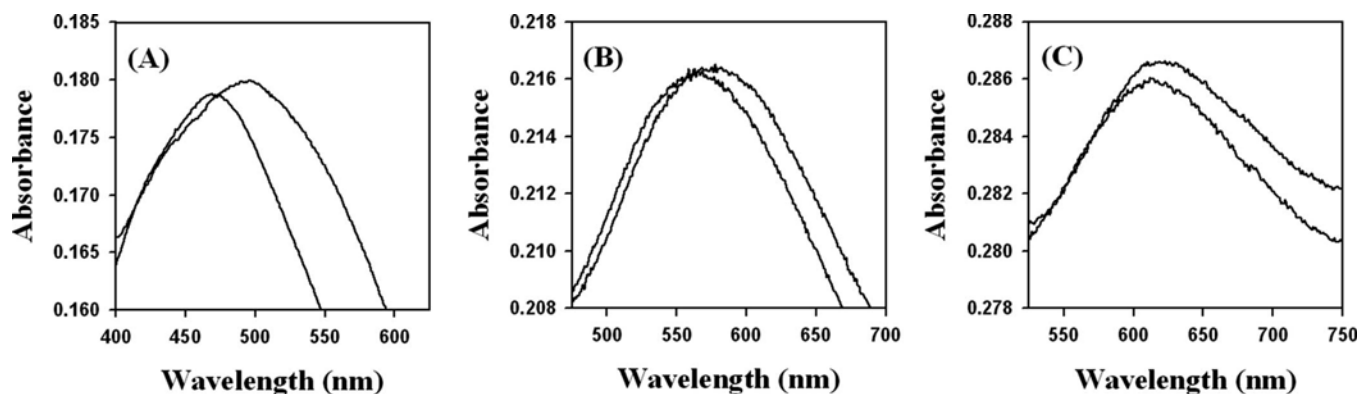
FIG. 5. UV/visible spectra of different diameter Ag nanoparticle sensor arrays before and after incubated with 1.0×10^{-6} M streptavidin solutions. The arrays employed (a) 34 nm, (b) 55 nm, and (c) 72 nm diameter Ag nanoparticles. The spectrum after adsorption is redshifted and slightly higher than the one before adsorption in each case.

fore, for practical sensor design, it appears that smaller nanoparticle sizes (at least down to 20 or 30 nm) appear to be more useful than larger ones.

The current results are in reasonable arrangement with previous studies by Nath and Chilkoti, where they found that nanoparticles with 39 nm diameters had optimal sensitivity. In that case, spherical Au nanoparticles were made in solution and subsequently loaded onto the substrate. Therefore, our half sphere-shaped Ag nanoparticle array would not necessarily be expected to yield identical results. Nevertheless, the need to tune both the adsorption and frequency shift probably lead to optimum performance in the range of a few tens of nanometers for nanoparticles, in general.

IV. DISCUSSION

Ideal biosensors should be extremely sensitive, highly selective, simple to fabricate, and easy to use. They should operate with tiny sample volumes in a label-free fashion with low background response. Surface plasmon resonance techniques have, at least in principle, many of these features, which would allow them to compare favorably with conventional labeling techniques such as fluorescence.[56] Moreover, T-LSPR should be easier to employ than reflectometry SPR because of its very simple setup. The combination of transmission mode detection, rapid metal nanoparticle fabrication, and surface passivation with a PEG-thiol appear to make this platform attractive.

It should be noted that Au and Ag nanoarchitectures are common motifs for plasmonic-based biosensors. Among the several T-LSPR experiments based on Au/Ag nanoparticles reported previously, two general strategies were employed to fabricate nanoparticle arrays on substrates. First, nanoparticles can be made in solution using standard procedures and loaded onto the substrate by specific linkage or nonspecific adsorption.[11,14] Alternatively, the nanoparticles can be directly fabricated *in situ* on the substrate.[12,21,22,62] The first method requires an extra step and the final surface coverage can be difficult to control. On the other hand, direct deposition can limit the variety of geometries of the particles and uniformity may be uneven. The present method is advantageous because it circumvents several of these problems. For example, the use of a template allows significant control over particle size, spacing, and geometry while still providing the convenience of a direct fabrication method. Indeed, the size distribution of our particles is narrow and the fabrication process can be performed rapidly.

ACKNOWLEDGMENTS

TABLE I. Maximum wavelength shifts ($\Delta\lambda_{max}$) with four different sizes of Ag nanoparticles.

Particle size FWHH (nm)	Maximum wavelength shift $\Delta\lambda_{max}$ (nm)	Absorbance at λ_{max}
19	24 ± 4	0.137
34	21 ± 3	0.179
55	12 ± 4	0.216
72	10 ± 2	0.285

[1] J. Homola, S. S. Yee, and G. Gauglitz, Sens. Actuators B **54**, 3 (1999).
[2] R. J. Green, R. A. Frazier, K. M. Shakesheff, M. C. Davies, C. J. Roberts, and S. J. B. Tendler, Biomaterials **21**, 1823 (2000).
[3] J. Homola, Anal. Bioanal. Chem. **377**, 528 (2003).
[4] A. J. Haes, C. L. Haynes, A. D. McFarland, G. C. Schatz, R. P. Van Duyne, and S. L. Zou, MRS Bull. **30**, 368 (2005).
[5] D. Roy and J. Fendler, Adv. Mater. (Weinheim, Ger.) **16**, 479 (2004).
[6] B. Rothenhäusler and W. Knoll, Nature (London) **332**, 615 (1988).
[7] B. P. Nelson, T. E. Grimsrud, M. R. Liles, R. M. Goodman, and R. M. Corn, Anal. Chem. **73**, 1 (2001).
[8] J. S. Shumaker-Parry, R. Aebersold, and C. T. Campbell, Anal. Chem. **76**, 2071 (2004).
[9] L. K. Wolf, D. E. Fullenkamp, and R. M. Georgiadis, J. Am. Chem. Soc. **127**, 17453 (2005).
[10] K. S. Phillips, T. Wilkop, J.-J. Wu, R. O. Al-Kaysi, and Q. Cheng, J. Am. Chem. Soc. **128**, 9590 (2006).
[11] T. Okamoto, I. Yamaguchi, and T. Kobayashi, Opt. Lett. **25**, 372 (2000).
[12] G. Kalyuzhny, A. Vaskevich, G. Ashkenasy, A. Shanzer, and I.

Rubinstein, J. Phys. Chem. B **104**, 8238 (2000).

[13]M. D. Malinsky, K. L. Kelly, G. C. Schatz, and R. P. Van Duyne, J. Am. Chem. Soc. **123**, 1471 (2001).

[14]N. Nath and A. Chilkoti, Anal. Chem. **74**, 504 (2002).

[15]Y.-S. Shon, H. Y. Choi, M. S. Guerrero, and C. Kwon, Plasmonics **4**, 95 (2009).

[16]M. P. Jonsson, A. B. Dahlin, P. Jönsson, and F. Höök, BioInterphases **3**, FD30 (2008).

[17]F. Frederix, J.-M. Friedt, K.-H. Choi, W. Laureyn, A. Campitelli, D. Mondelaers, G. Maes, and G. Borghs, Anal. Chem. **75**, 6894 (2003).

[18]N. Nath and A. Chilkoti, Anal. Chem. **76**, 5370 (2004).

[19]L. J. Sherry, R. Jin, C. Mirkin, G. C. Schatz, and R. P. Van Duyne, Nano Lett. **6**, 2060 (2006).

[20]U. Kreibig and M. Vollmer, *Optical Properties of Metal Clusters* (Springer, Heidelberg, 1995), Vol. 25.

[21]G. Kalyuzhny, A. Vaskevich, M. A. Schneeweiss, and I. Rubinstein, Chem.-Eur. J. **8**, 3849 (2002).

[22]I. Doron-Mor, H. Cohen, Z. Barkay, A. Shanzer, A. Vaskevich, and I. Rubinstein, Chem.-Eur. J. **11**, 5555 (2005).

[23]I. Ruach-Nir, T. A. Bendikov, I. Doron-Mor, Z. Barkay, A. Vaskevich, and I. Rubinstein, J. Am. Chem. Soc. **129**, 84 (2007).

[24]S. M. Marinakos, S. Chen, and A. Chilkoti, Anal. Chem. **79**, 5278 (2007).

[25]G. J. Nusz, S. M. Marinakos, A. C. Curry, A. Dahlin, F. Höök, A. Wax, and A. Chilkoti, Anal. Chem. **80**, 984 (2008).

[26]K. M. Mayer, S. Lee, H. Liao, B. C. Rostro, A. Fuentes, P. T. Scully, C. L. Nehl, and J. H. Hafner, ACS Nano **2**, 687 (2008).

[27]A. Dahlin, M. Zäch, T. Rindzevicius, M. Käll, S. D. Sutherland, and F. Höök, J. Am. Chem. Soc. **127**, 5043 (2005).

[28]J. C. Sharpe, J. S. Mitchell, L. Lin, N. Sedoglavich, and R. J. Blaikie, Anal. Chem. **80**, 2244 (2008).

[29]A. G. Brolo, R. Gordon, B. Leathem, and K. L. Kavanagh, Langmuir **20**, 4813 (2004).

[30]A. G. Brolo, S. C. Kwok, M. D. Cooper, M. G. Moffitt, C.-W. Wang, R. Gordon, J. Riordon, and K. L. Kavanagh, J. Phys. Chem. B **110**, 8307 (2006).

[31]A. J. Haes and R. P. Van Duyne, J. Am. Chem. Soc. **124**, 10596 (2002).

[32]K. Hutter and M.-P. Pileni, J. Phys. Chem. B **107**, 6497 (2003).

[33]J. Spadavecchia, P. Prete, N. Lovergine, L. Tapfer, and R. Rella, J. Phys. Chem. B **109**, 17347 (2005).

[34]I. Tokareva, S. Minko, J. H. Fendler, and E. Hutter, J. Am. Chem. Soc. **126**, 15950 (2004).

[35]W.-S. Liao, T. Yang, E. T. Castellana, S. Kataoka, and P. S. Cremer, Adv. Mater. (Weinheim, Ger.) **18**, 2240 (2006).

[36]M. R. Hoffmann, S. T. Martin, W. Y. Choi, and D. W. Bahnemann, Chem. Rev. (Washington, D.C.) **95**, 69 (1995).

[37]S. Nishimoto, B. Ohtani, H. Kajiwara, and T. Kagiya, J. Chem. Soc., Faraday Trans. I **79**, 2685 (1983).

[38]M. R. V. Sahyun and N. Serpone, Langmuir **13**, 5082 (1997).

[39]M. I. Litter, Appl. Catal., B **23**, 89 (1999).

[40]E. Szabo-Bardos, H. Czili, and A. Horvath, J. Photochem. Photobiol., A **154**, 195 (2003).

[41]D. Shchukin, E. Ustinovich, D. Sviridov, and P. Pichat, Photochem. Photobiol. Sci. **3**, 142 (2004).

[42]F. X. Zhang, N. J. Guan, Y. Z. Li, X. Zhang, J. X. Chen, and H. S. Zeng, Langmuir **19**, 8230 (2003).

[43]E. T. Castellana, S. Kataoka, F. Albertorio, and P. S. Cremer, Anal. Chem. **78**, 107 (2006).

[44]E. Stathatos, P. Lianos, P. Falaras, and A. Siokou, Langmuir **16**, 2398 (2000).

[45]J. He, I. Ichinose, S. Fuikawa, T. Kunitake, and A. Nakao, Chem. Commun. (Cambridge) **2002**, 1910.

[46]K. Zakrzewska, M. Radecka, A. Kruk, and W. Osuch, Solid State Ionics **157**, 349 (2003).

[47]K. L. Kelly, E. Coronado, L. Zhao, and G. C. Schatz, J. Phys. Chem. B **107**, 668 (2003).

[48]I. O. Sosa, C. Noguez, and R. G. Barrera, J. Phys. Chem. B **107**, 6269 (2003).

[49]E. J. Zeman and G. C. Schatz, J. Phys. Chem. **91**, 634 (1987).

[50]D. D. Evanoff, Jr. and G. Chumanov, J. Phys. Chem. B **108**, 13948 (2004).

[51]A. S. Kumbhar, M. K. Kinnan, and G. Chumanov, J. Am. Chem. Soc. **127**, 12444 (2005).

[52]R. C. Jin, Y. C. Cao, E. C. Hao, G. S. Me'traux, G. C. Schatz, and C. A. Mirkin, Nature (London) **425**, 487 (2003).

[53]Y. Sun and Y. Xia, Adv. Mater. (Weinheim, Ger.) **15**, 695 (2003).

[54]R. C. Jin, Y. C. Cao, C. A. Mirkin, K. L. Kelly, G. C. Schatz, and J. G. Zheng, Science **294**, 1901 (2001).

[55]A. Chilkoti and P. S. Stayton, J. Am. Chem. Soc. **117**, 10622 (1995).

[56]E. A. Smith, W. D. Thomas, L. L. Kiessling, and R. M. Corn, J. Am. Chem. Soc. **125**, 6140 (2003).

[57]L. S. Jung, K. E. Nelson, P. S. Stayton, and C. T. Campbell, Langmuir **16**, 9421 (2000).

[58]K. E. Nelson *et al.*, Langmuir **17**, 2807 (2001).

[59]V. H. Pérez-Luna, M. J. O'Brien, K. A. Opperman, P. D. Hampton, G. P. López, L. A. Klumb, and P. S. Stayton, J. Am. Chem. Soc. **121**, 6469 (1999).

[60]N. M. Green, Adv. Protein Chem. **29**, 85 (1975).

[61]G. J. Nusz, A. C. Curry, S. M. Marinakos, A. Wax, and A. Chilkoti, ACS Nano **3**, 795 (2009).

[62]G. Kalyuzhny, M. A. Schneeweiss, A. Shanzer, A. Vaskevich, and I. Rubinstein, J. Am. Chem. Soc. **123**, 3177 (2001).